Distal Degenerative Sensory Neuropathy in a Long-Term Type 2 Diabetes Rat Model

Valentine Brussee,[1] GuiFang Guo,[1] YingYing Dong,[1] Chu Cheng,[1] José A. Martinez,[1] Darrell Smith,[2,3] Gordon W. Glazner,[2,3] Paul Fernyhough,[2,3] and Douglas W. Zochodne[1]

OBJECTIVE—Peripheral neuropathy associated with type 2 diabetes (DPN) is not widely modeled. We describe unique features of DPN in type 2 diabetic Zucker diabetic fatty (ZDF) rats.

RESEARCH DESIGN AND METHODS—We evaluated the structural, electrophysiological, behavioral, and molecular features of DPN in ZDF rats and littermates over 4 months of hyperglycemia. The status of insulin signaling transduction molecules that might be interrupted in type 2 diabetes and selected survival-, stress-, and pain-related molecules was emphasized in dorsal root ganglia (DRG) sensory neurons.

RESULTS—ZDF rats developed slowing of motor sciatic-tibial and sensory sciatic digital conduction velocity and selective mechanical allodynia with preserved thermal algesia. Diabetic sural axons, preserved in number, developed atrophy, but there was loss of large-calibre dermal and small-calibre epidermal axons. In diabetic rats, insulin signal transduction pathways in lumbar DRGs were preserved or had trends toward upregulation: mRNA levels of insulin receptor β-subunit (IRβ), insulin receptor substrate (IRS)-1, and IRS-2. The numbers of neurons expressing IRβ protein were also preserved. There were trends toward early rises of mRNA levels of heat shock protein 27 (HSP27), the α2δ1 calcium channel subunit, and phosphatidylinositol 3-kinase in diabetes. Others were unchanged, including nuclear factor-κB (NF-κB; p50/p105) and receptor for advanced glycosylation endproducts (RAGE) as was the proportion of neurons expressing HSP27, NF-κB, and RAGE protein.

CONCLUSIONS—ZDF type 2 diabetic rats develop a distal degenerative sensory neuropathy accompanied by a selective long-term pain syndrome. Neuronal insulin signal transduction molecules are preserved. ***Diabetes*** **57:1664–1673, 2008**

From the [1]Department of Clinical Neurosciences and the Hotchkiss Brain Institute, University of Calgary, Calgary, Alberta, Canada; the [2]Division of Neurodegenerative Disorders, St. Boniface Hospital Research Centre, Winnipeg, Canada; and the [3]Department of Pharmacology and Therapeutics, University of Manitoba, Winnipeg, Canada.

Corresponding author: Dr. D.W. Zochodne, University of Calgary, 3330 Hospital Dr. NW, Calgary, Alberta T2N 4N1, Canada. E-mail: dzochodn@ucalgary.ca.

Received for publication 12 December 2007 and accepted in revised form 29 February 2008.

Published ahead of print at http://diabetes.diabetesjournals.org on 10 March 2008. DOI: 10.2337/db07-1737.

AHFMR, Alberta Heritage Foundation for Medical Research; C_T, threshold cycle; DPN, peripheral polyneuropathy; DRG, dorsal root ganglia; HKG, housekeeping gene; HSP27, heat shock protein 27; IRβ, insulin receptor β-subunit; IRS, insulin receptor substrate; NF-κB, nuclear factor-κB; PI 3-kinase, phosphatidylinositol 3-kinase; RAGE, receptor for advanced glycosylation endproducts; STZ, streptozotocin; ZDF, Zucker diabetic fatty.

The World Health Organization estimates that 366 million people worldwide (up from 171 million in 2000) will suffer from diabetes by the year 2030 (1). Most have type 2 diabetes and about one-half have evidence of peripheral polyneuropathy (DPN). Attention toward the mechanisms of DPN has largely focused on type 1 models, for example, after streptozotocin (STZ)-induced β-cell damage in rats and mice. In long-term type 1 models, however, important insights into the human disease have emerged. These have suggested a chronic neurodegenerative condition with gradual loss of distal motor and sensory terminals and features of neuropathic pain (2–7). The upregulation of selected "stress"-related neuronal molecules may or may not accompany frank neuronal loss, depending on the model (7,8).

Work using type 2 diabetic animal models has been carried out but less frequently (9–11). These models are more expensive to maintain and only rarely are carried out to longer time points. One important question is whether this model exhibits features of DPN that include a progressive degenerative disorder manifested as selective loss and abnormality of distal terminal axons. Neuropathic pain is a critical element of the DPN phenotype but whether both thermal hyperalgesia and mechanical allodynia develop concurrently has been debated. Type 1 DPN models also exhibit heightened expression of insulin receptors in lumbar dorsal root ganglia (DRG) and sensitivity to its action, even at low subhypoglycemic doses (12–15). Whether insulin signaling transduction machinery is preserved or downregulated in a type 2 DPN model where initial high circulating insulin levels occur is of interest. Finally, it is uncertain whether alterations in select neuronal indexes of neurotoxic stress observed in type 1 diabetes also occur in a longer term type 2 model.

In this work, we examine a long-term model of type 2 DPN, that of the Zucker diabetic fatty (ZDF) rat first described in work by Peterson and colleagues (16) and by Shaw and colleagues (17). Male obese ZDF (*fa/fa* or ZDF/Drt-fa; Charles River) are homozygous for a missense mutation causing a nonfunctional leptin receptor (*fa/fa*), and control littermates are heterozygous (*fa*/+) lean males (18). ZDF rats develop obesity, initial hyperinsulinemia (insulin resistance), and then pancreatic failure with overt diabetes after 8–10 weeks (19). Several papers have described neurological features, including slowing of conduction velocity (10,11,20–22), alterations in sensory testing (10,21), and differences from the long-term STZ model in autonomic ganglia (23). Here, we evaluate the impact of type 2 diabetes on the phenotype and expression patterns of sensory neurons. The findings suggest a distal degenerative disorder resembling that of type 1 DPN, with

selective pain behavior and preserved insulin signal transduction machinery.

RESEARCH DESIGN AND METHODS

Diabetes model. Rats were purchased from Charles River Laboratories (Wilmington, MA) and shipped to the University of Calgary or University of Manitoba at 6 weeks of age. Cohorts were obese diabetic male ZDF/crl-lepr/fa and control male lean *fa*/+. The onset of hyperglycemia was determined by weekly urine testing after receipt and developed at ~8 weeks of age. The rats were raised on Purina rat chow 5008. Blood glucose levels were measured using a glucose strip tester (One Touch Ultra; Lifescan, Johnson and Johnson, Burnaby, BC, Canada). All invasive procedures were carried out under 65 mg/kg pentobarbital anesthesia. The protocols were reviewed and approved by the University of Calgary and University of Manitoba Animal Care Committees using the Canadian Council of Animal Care guidelines.

Electrophysiology/pain behavior testing. Motor conduction in sciatic-tibial fibers was performed by stimulating at the sciatic notch and knee while recording the M-wave (compound muscle action potential) from the tibial-innervated dorsal interossei foot muscles. Digital sciatic-tibial sensory conduction was made by stimulation of the digital nerves of the paw and recording over the sciatic nerve at the level of the popliteal fossa. All stimulating and recording used platinum subdermal needle electrodes (Grass Instruments; Astro-Med, West Warwick, RI) with near nerve temperature kept constant at 37 ± 0.5°C using a heating lamp.

Mechanical withdrawal frequencies were measured using calibrated (4–26 g) von Frey monofilaments (Stoelting, Wood Dale, IL) applied to the dorsum of the paw to a rat habituated within a plexiglass cage with holes in the flooring to allow application. Each paw was probed three times for ~1 s to the plantar surface with enough force to cause slight flexion of the monofilament, and the amount of withdrawal was graded at 0 (none) to 2 (maximum) for each probe. Summing these grades bilaterally yielded values ranging from 0 (no withdrawal to any of the probes) to 6 (maximum withdrawal to each probe), corresponding then to withdrawal percentages of 0–100%. For thermal sensitivity, the latency of withdrawal of the hindpaw to an applied heat using the Hargreaves apparatus stimulus (24) was measured, and the sum of the right and left latency was calculated.

Morphometry. Sural nerves were harvested and processed as described in previous work (2). Samples were fixed in 2.5% glutaraldehyde in 0.025 mol/l cacodylate buffer overnight. Semithin (1-μm) sections of sural nerve and lumbar L4–6 DRGs were cut on an ultramicrotome (Reichert, Vienna, Austria) and were stained with toluidine blue. Morphometric analysis was carried out using a Zeiss Axioskop at magnification ×1,000. Computer-assisted image analysis allowed for the determination of number and caliber of intact myelinated fibers. All morphological measurements were performed using Scion Image v.4.0.2 (Scion, Frederick, MD) by a single microscopist blinded to origin of the samples.

Immunohistochemistry. L5 DRGs were harvested, fixed in Zamboni's preparation, and mounted in Optimal Cutting Temperature (Tissue-Tek, Sakura-Finetek, Torrance, CA). Cryostat sections (14 μm for DRG samples) were immunostained with primary antibodies: rabbit polyclonal antibody against insulin receptor β-subunit (IRβ [C-19]; 1:100; Santa Cruz); rabbit polyclonal antibody to heat shock protein 27 (HSP27) (1:1,000; Stressgen Biotechnologies, San Diego, CA); rabbit polyclonal antibody to human receptor for advanced glycosylation endproducts (RAGE; 1:100; gift from Dr. A.M. Schmidt, Columbia University NY); rabbit polyclonal antibody to nuclear factor-κB (NF-κB p50 subunit [H-119]; 1:100; Santa Cruz). For skin sections (25 μm thickness), we used a rabbit polyclonal antibody to PGP9.5 (1:1,000; Cedarlane, Burlington, Ontario, Canada). Nonspecific staining was blocked using 1% goat serum (excepting PGP9.5, which used 10%). Secondary antibodies were anti-goat and -rabbit 488 (1:400; Invitrogen, Carlsbad, CA) and donkey anti-goat 488 (1:200; Invitrogen).

All analysis was conducted with the examiner blinded to the identity of the samples being studied. Neurons were counted in three sections through the midportion of the DRG to determine the total neuron numbers per transverse section and the total number and percentage of neurons labeled with HSP27, RAGE, and IRβ. Neurons with an arbitrary measurement of luminosity >70 were classified as immunoreactive. We also classified neurons as none–low (0–100), moderate (101–200), or high (>200) using Adobe Photoshop software version 7.0 (Adobe, San Jose, CA). Specifically for NF-κB p50, we examined three sections through the midportion of the DRG and determined the mean total neuron number per transverse section, the mean number of neurons with nuclei per transverse section, and the total number (and percentage) of neurons labeled with NF-κB p50 subunit with luminosity >70 (including that of the cytoplasm, nucleus, or both). A caveat to the analysis was that nuclei in general were more likely to be identified if labeled, probably falsely elevating the overall percent of positive nuclei in both groups. We calculated the percentage of positive nuclei out of the total number of nuclei identified for both groups. For footpads, dermal analysis was carried out after labeling with an antibody to Nf200, the heavy subunit of neurofilament (mouse monoclonal anti-Nf200; 1:200; Sigma, St. Louis, MO). Six fields per section and four sections per animal underwent quantitative analysis: Both live images and computer-captured images were used for counting, but live images were preferred for the analysis. A mean value per rat and per test group was calculated.

The epidermal fibers were counted in six sections per rat (5 papillae fields were examined in each section for a total of 30 papillae per rat), and we determined the number of epidermal fibers including axons directed vertically or horizontally (separately or combined). We measured the areas (mm^2) for each papilla using Image J software (National Institutes of Health, Bethesda, MD). Images were captured using an Olympus laser scanning Confocal microscope equipped with epifluorescence magnification ×60, and the scanning step size was 1 μm.

Quantitative RT-PCR. Real-time quantitative RT-PCR was performed on the ABI Prism 7000 sequence detection system (Applied Biosystems, Foster City, CA). Total RNA was extracted from rat lumbar L3 and L6 DRG using TRIzol reagent according to the manufacturer's protocol (Invitrogen). One microgram DNase 1–treated total RNA was used to synthesize first-strand DNA using SuperScript II First-strand Synthesis kit (Invitrogen). Random hexamers (0.9 μg) were used as per the manufacturer's protocol. First-strand DNA (0.05 μl) was then used for PCR reactions. Quantification of the amplified product was done on a cycle-by-cycle basis through the acquisition of a fluorescent signal generated by binding of the fluorophore SybrGreen I (Invitrogen) to double-stranded DNA. The cycle number was determined at which the fluorescence signal crossed a fixed threshold (threshold cycle [C_T]). The volume of the PCR mixture was 30 μl comprising 1 unit *Taq*DNA polymerase

TABLE 1
Primer sequences

Cyclophilin forward	5′-TGTGCCAGGGTGGTGACTT-3′
Cyclophilin reverse	5′-TCAAATTTCTCTCCGTAGATGGACTT-3′
18S rRNA forward	5′-TCCCTAGTGATCCCCGAGAAGT-3′
18S rRNA reverse	5′-CCCTTAATGGCAGTGATAGCGA-3′
IRβ forward	5′-CTGAAGGAGCTGGAGGAGTC-3′
IRβ reverse	5′-GATTTCATGGGTCACAGGGC-3′
IRS-1 forward	5′-AACCGCAAAGGAAATGGGGACTAT-3′
IRS-1 reverse	5′-CTGCGCTGATGCTGCTACTGCT-3′
IRS-2 forward	5′-AGAACCCAGACCCTAAGCTGCT-3′
IRS-2 reverse	5′-CGCAAAGCTGCTGAGAAGAAG-3′
PI 3-kinase forward	5′-AACGTCATGAGGCGCTTCA-3′
PI 3-kinase reverse	5′-TGCACCAGGCGATCTACAAA-3′
AKT reverse	5′-TTTGTCATGGAGTACGCCAATG-3′
AKT forward	5′-CACAATCTCCGCACCGTAGAA-3′
NF-κB (p50/p105) forward	5′-CATGGTGGTTGGCTTTGCA-3′
NF-κB (p50/p105) forward	5′-AGCCCCTAATACACGCCTCTGT-3′
RAGE forward	5′-GGAAGGACTGAAGCTTGGAAGG-3′
RAGE reverse	5′-TCCGATAGCTGGAAGGAGGAGT-3′
HSP27 forward	5′-GAAATACACGCTCCCTCCAGGT-3′
HSP27 reverse	5′-TCCGCTGATTGTGTGACTGCT-3′

TABLE 2
Weights

Group	Weight	Glucose
Control 1 month	301 ± 4 (19)	4.5 ± 0.2 (15)
Control 4 months	447 ± 8 (18)	
Diabetes baseline		4.5 ± 0.3 (15)
Diabetes 1 month	334 ± 6 (23)*	10.0 ± 0.6 (15)
Diabetes 4 months	397 ± 10 (19)†	12.6 ± 0.9 (15)

Data are means ± SE. ANOVA, $P < 0.0001$. *Diabetic rat vs. control, $P < 0.01$. †Diabetic rat vs. control, $P < 0.001$ (Tukey's multiple comparison test post-ANOVA).

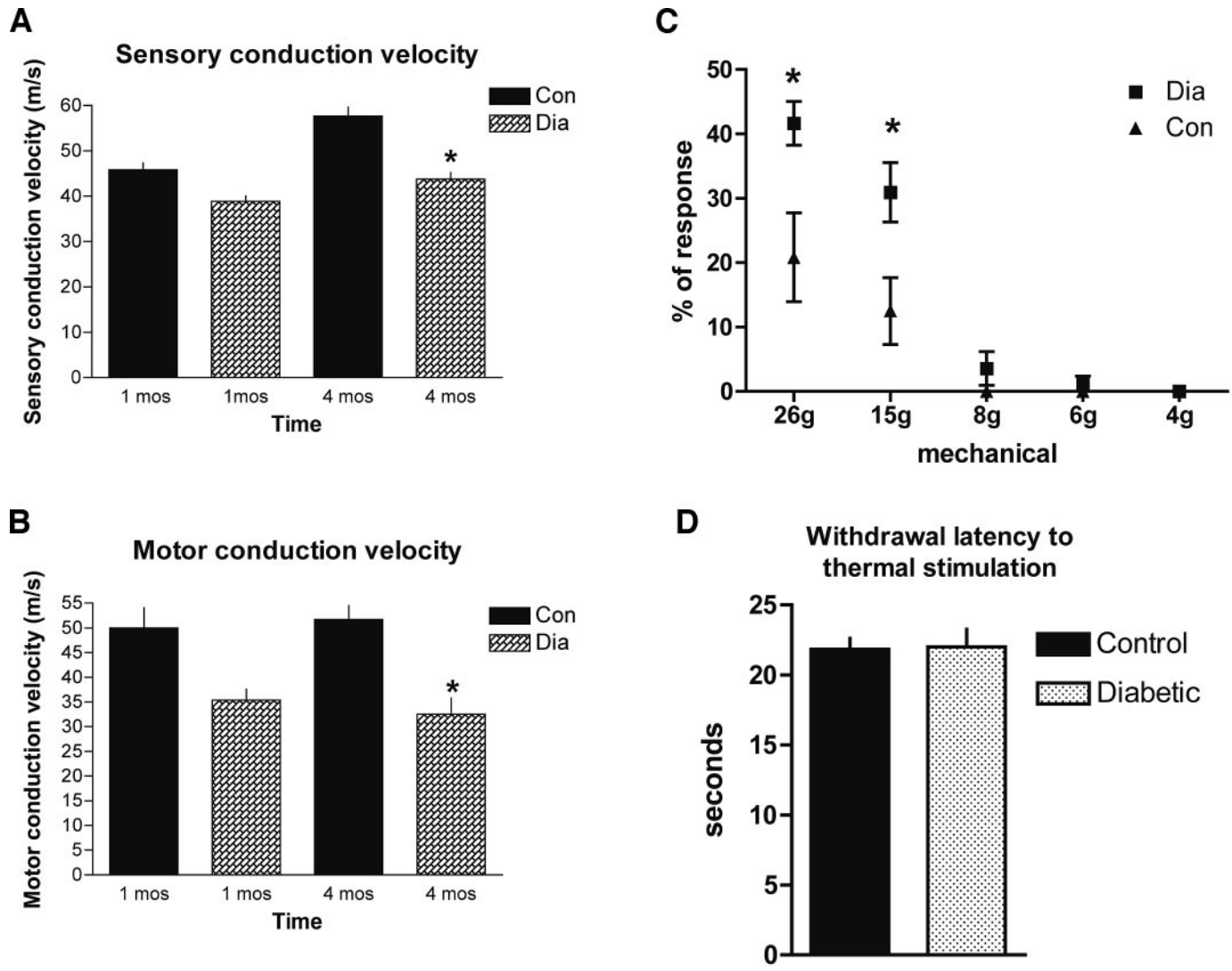

FIG. 1. Electrophysiological recordings and measurements of pain sensation. *A*: Measurements of conduction velocity in sciatic-tibial sensory axons. ZDF type 2 diabetic rats exhibited slowing of conduction at 4 months after the onset of diabetes (*$P < 0.001$ diabetic vs. control; control, $n = 13$ for month 1 and $n = 11$ for month 4; diabetic rats, $n = 4$ for month 1 and $n = 15$ for month 4). *B*: Measurements of conduction velocity in sciatic-tibial motor axons. ZDF type 2 diabetic rats exhibited slowing of conduction at 4 months after the onset of diabetes (*$P < 0.001$ diabetic vs. control; control, $n = 14$ for month 1 and $n = 11$ for month 4; diabetic rats, $n = 4$ for month 1 and $n = 15$ for month 4). *C*: Measurements of sensitivity to mechanical stimulation in the sole of the hindpaw. ZDF type 2 diabetic rats (DI) had a greater sensitivity to von Frey hair stimulation at 26 and 15 g than control littermates, indicating allodynia (*$P < 0.02$ diabetic vs. control; controls, $n = 8$; diabetic rats, $n = 14$). *D*: Measurements of sensitivity to thermal stimulation in the sole of the hindpaw. There was no difference in the withdrawal latencies between diabetic rats and controls (controls, $n = 8$; diabetic rats, $n = 14$).

mixture (Invitrogen), 3 mmol/l $MgCl_2$, 1.25 μmol/l concentrations of primers of interest (Invitrogen), and 5 μl cDNA. The amplification programs were performed as follows: *1*) heating at 95°C for 10 min; *2*) 40 cycles of 95°C for 15 s and 60°C for 1 min. A melting curve was acquired by heating the product, and the fluorescent signal was collected as the last step to look for a signal from nonspecific products, particularly from primer dimers. The standards and the samples tested were run in duplicate. Amplification of the product was visualized in the quantification curve analysis. The primer sequences used were designed in Primer Express 2.0 (Applied Biosystems) and are given in Table 1. The unknown samples are compared against the calibrator sample to give relative gene expression using the comparative C_T method $2^{-\Delta\Delta C}{}_T$. Final results were analyzed by choosing cyclophilin as the housekeeping gene (HKG) and separately analyzing both the L3 and the L6 ganglia. As an additional control, we also completed all assays using a second HKG, the 18s subunit of rRNA. In the case of mRNAs demonstrating changes or trends toward changes, we were able to confirm that similar directions of change were also observed when using 18S rRNA. In the case of both HSP27 and insulin receptor substrate (IRS)-2, upregulation was approximately twofold or greater in DRG from diabetic rats irrespective of the HKG or ganglia chosen, a consistent result that we interpreted as meaningful.

Analysis. Data were calculated as means ± SE. Data were analyzed by one-way ANOVA with Tukey's multiple comparison post hoc test or using two-tailed Student's *t* test comparisons (unless otherwise stated). In all tests, statistical significance was set at 0.05.

RESULTS

Model. Diabetic rats developed significant and progressive hyperglycemia from baseline to 1 and 4 months of diabetes duration. At 1 month, ZDF diabetic rats had a greater weight than controls, but by the 4-month end point, nondiabetic lean control rats had a greater weight. Weights and glucose levels are given in Table 2.

Progressive conduction slowing. Diabetic rats developed progressive and significant slowing of both motor sciatic-tibial and sciatic digital sensory conduction velocities between the 1- and 4-month end points. There was a trend toward slower motor and sensory conduction in diabetic rats compared with nondiabetic littermates by 1 month that was significant by 4 months. Results are given in Fig. 1*A* and *B*. The amplitudes of the compound muscle

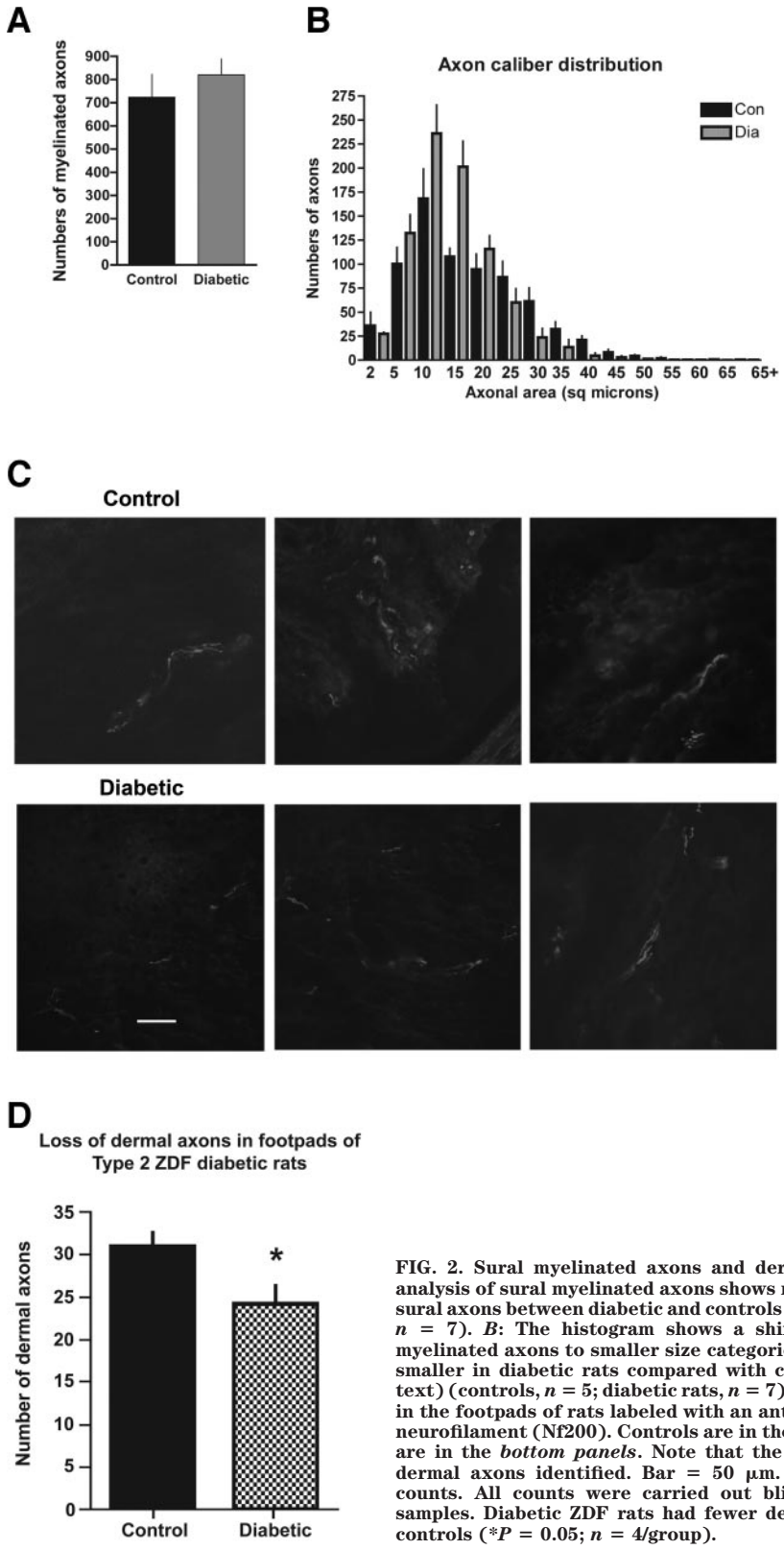

FIG. 2. Sural myelinated axons and dermal axons. *A*: Morphometric analysis of sural myelinated axons shows no difference in the number of sural axons between diabetic and controls (controls, $n = 5$; diabetic rats, $n = 7$). *B*: The histogram shows a shift in the calibre of diabetic myelinated axons to smaller size categories. The mean axonal area was smaller in diabetic rats compared with controls (data not shown; see text) (controls, $n = 5$; diabetic rats, $n = 7$). *C*: Examples of dermal axons in the footpads of rats labeled with an antibody to the heavy subunit of neurofilament (Nf200). Controls are in the *top panels*, and diabetic rats are in the *bottom panels*. Note that the diabetic samples have fewer dermal axons identified. Bar = 50 μm. *D*: Analysis of dermal axon counts. All counts were carried out blinded to the identity of the samples. Diabetic ZDF rats had fewer dermal axons than nondiabetic controls (*$P = 0.05$; $n = 4$/group).

action potentials and sensory nerve action potentials did not differ between diabetic rats and nondiabetic controls (data not shown).

Selective development of mechanical allodynia. Diabetic rats demonstrated mechanical allodynia at the 4-month end point as illustrated by higher withdrawal scores to von Frey hair stimulation at the two highest of the five stimulus intensities studied (Fig. 1*C*). The thermal withdrawal latency did not differ between diabetic and nondiabetic rats at the 4-month end point (Fig. 1*D*). Overall, the findings confirmed a selective phenotype of pain behavior in diabetic rats.

Retraction of distal sensory terminals. The number of myelinated axons or fibers in the sural nerve was compa-

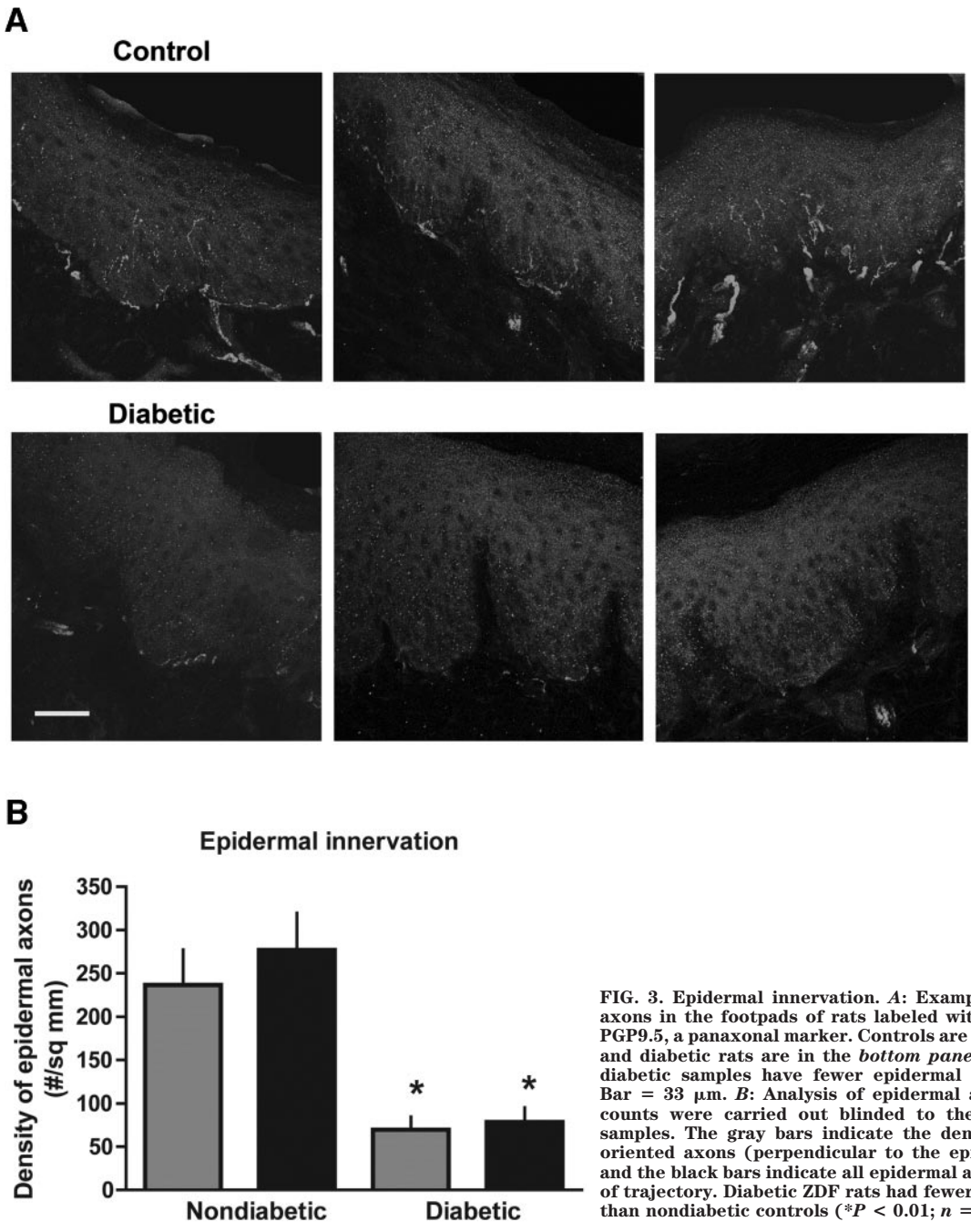

FIG. 3. Epidermal innervation. *A*: Examples of epidermal axons in the footpads of rats labeled with an antibody to PGP9.5, a panaxonal marker. Controls are in the *top panels*, and diabetic rats are in the *bottom panels*. Note that the diabetic samples have fewer epidermal axons identified. Bar = 33 μm. *B*: Analysis of epidermal axon density. All counts were carried out blinded to the identity of the samples. The gray bars indicate the density of vertically oriented axons (perpendicular to the epidermal surface), and the black bars indicate all epidermal axons irrespective of trajectory. Diabetic ZDF rats had fewer epidermal axons than nondiabetic controls (*$P < 0.01$; $n = 6$/group).

rable between diabetic and nondiabetic rats (Fig. 2*A*). Diabetic sural nerve axons demonstrated axonal atrophy with shifts of myelinated fibers to smaller axon size categories (Fig. 2*B*). The mean axonal area was 15.0 ± 1.0 μm^2 ($n = 5$) in controls and 11.9 ± 1.1 μm^2 ($n = 7$) in diabetic rats; $P = 0.04$, one-tailed Student's t test).

In contrast to sural axon counts, analysis of large axon innervation of the dermis of the foot pad using an antibody directed against neurofilament (Nf200) illustrated reductions in diabetic rats (Fig. 2*C* and *D*). The most terminal portions of the sensory axons in the epidermis were labeled with PGP9.5. In diabetic rats, there was a reduction of the density of epidermal axons (Fig. 3*A* and *B*).

Sensory neuron expression of insulin receptor signal transduction pathway. In other models of DPN and after axotomy injury to a peripheral branch of a sensory neuron, expression of insulin receptors increases and renders the associated signaling pathways more sensitive to the trophic properties of the peptide. We measured overall mRNA levels of three key elements of the insulin receptor signal transduction pathway by quantitative RT-PCR: IRβ, IRS-1, and IRS-2 (Fig. 4*A*). The mRNA levels of L6 DRGs had nonsignificant trends toward higher IRβ in diabetic rats than nondiabetic rats. The mRNA levels of IRS-1 also demonstrated a nonsignficant trend toward higher levels in diabetic L6 DRGs. For IRS-2, there were trends toward rises in its relative mRNA expression in L6 ganglia and a significant rise in its expression in the L3 ganglia. To address the proportion of neurons expressing IRβ, one of the subunits of the insulin receptor, we counted the proportion of sensory DRG neurons with low, medium, or high intensity expression by immunohistochemistry. There was

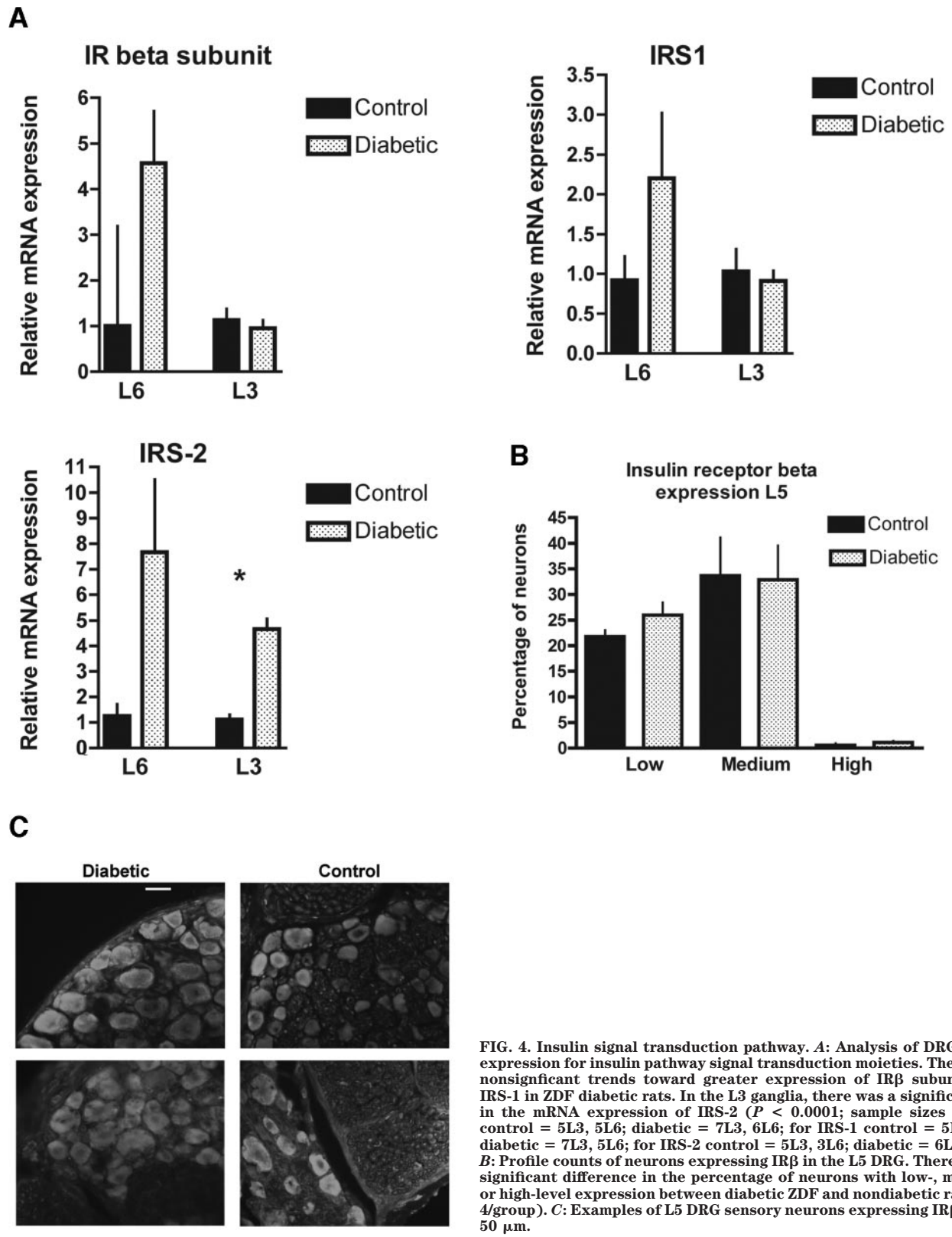

FIG. 4. Insulin signal transduction pathway. *A*: Analysis of DRG mRNA expression for insulin pathway signal transduction moieties. There were nonsignficant trends toward greater expression of IRβ subunits and IRS-1 in ZDF diabetic rats. In the L3 ganglia, there was a significant rise in the mRNA expression of IRS-2 ($P < 0.0001$; sample sizes for IRβ control = 5L3, 5L6; diabetic = 7L3, 6L6; for IRS-1 control = 5L3, 6L6; diabetic = 7L3, 5L6; for IRS-2 control = 5L3, 3L6; diabetic = 6L3, 5L6). *B*: Profile counts of neurons expressing IRβ in the L5 DRG. There was no significant difference in the percentage of neurons with low-, medium-, or high-level expression between diabetic ZDF and nondiabetic rats (n = 4/group). *C*: Examples of L5 DRG sensory neurons expressing IRβ. Bar = 50 μm.

no difference in the percentage of neurons expressing IRβ at the varying ranges of intensity (Fig. 4*B* and *C*).

Sensory neuron expression of selected survival- and stress-related pathways. There are a number of survival and protective molecules that are upregulated in other models of DPN, including HSP27, phosphatidylinositol 3-kinase (PI 3-kinase), and Akt. RAGE and NF-κB have been linked to cell damage but also to survival and are also upregulated in other models of DPN (25,26). To address their expression, we measured overall mRNA levels and counted sensory neurons expressing selected marker proteins. We identified trends toward rises in RAGE, NF-κB [p50/p105] (borderline trend), and the α2δ-1 calcium channel subunit mRNAs in L6 ganglia (but not L3) of diabetic

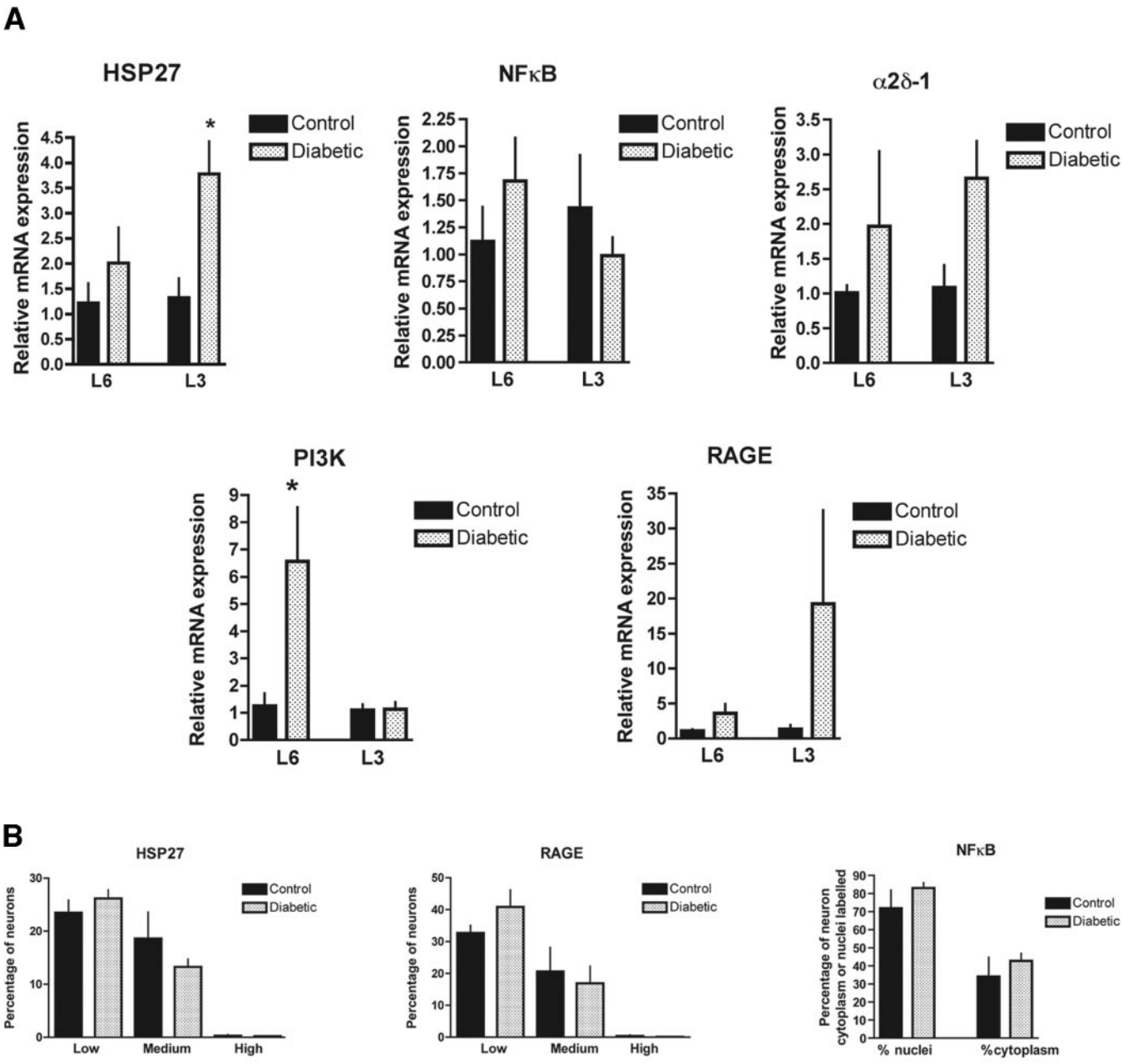

rats (Fig. 5*A*). NF200, calcitonin gene-related peptide, caspase-3, Akt, and GLUT4 mRNAs were not significantly different between diabetic and control animals (data not shown). There was a significant rise in the mRNA expression of PI 3-kinase in L6. For HSP27, there were rises in its relative mRNA expression in the L3 ganglia and a trend toward an increase in the L6 ganglia.

The percentage of L5 DRG sensory neurons expressing HSP27 and RAGE proteins at low-, medium-, and high-intensity levels detected using immunohistochemistry were comparable between diabetic and nondiabetic rats (Fig. 5*B* and *C*). For NF-κB p50 subunit, there were nonsignificant trends toward a rise in the percentage of neurons expressing this protein in either the L5 DRG cytoplasm or nucleus (Fig. 5*B* and *C*).

DISCUSSION

In this work, we first confirmed that a long-term type 2 diabetic animal model exhibits progressive nerve conduction slowing, an electrophysiological feature of DPN in rats, mice, other models, and humans. Second, we confirmed that pain behavior is a feature of this model, as in humans, but that it was both modality specific and present at a long-term end point. Third, we demonstrated that DPN is a distal neurodegenerative disorder with involvement of dermal and epidermal axons but preservation of proximal components of the sensory axis. Fourth, we showed that insulin signal transduction pathways are preserved or upregulated in the sensory neurons of this model. Finally, we suggest that there may also be early alterations in mRNAs of selected neuronal "stress" and survival pathways in this model.

The electrophysiological findings confirm the place of this model among others with similar findings. Unlike the STZ-induced type 1–like model, both hyperglycemia and conduction slowing develop more gradually. Progressive declines in compound muscle action potentials and sensory nerve action potentials were not observed but have

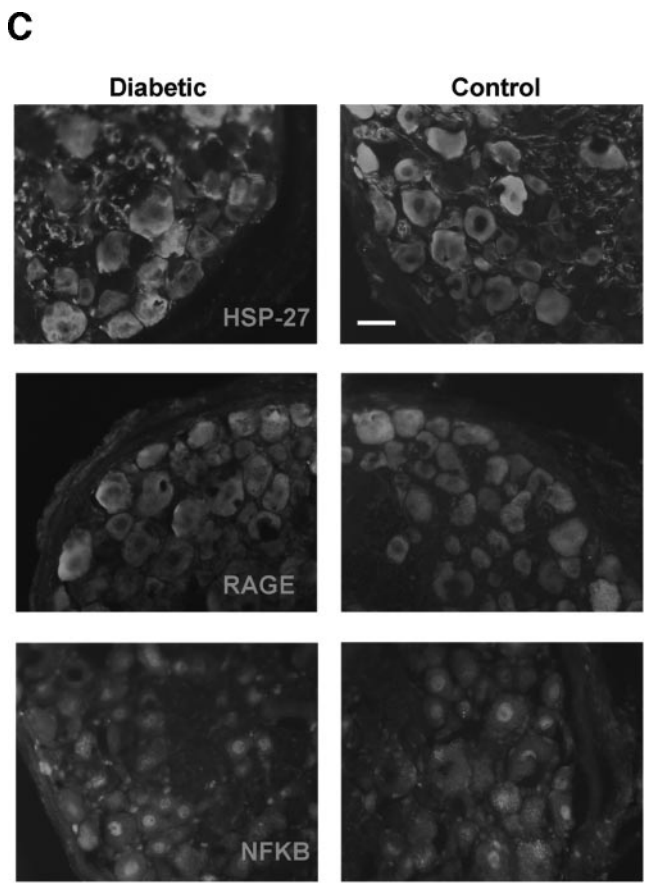

FIG. 5. Survival and stress pathways. *A*: Analysis of DRG mRNA expression for survival, stress, and pain molecules involving neurons. Significant rises were identified in HSP27 mRNAs of L3 neurons (*P = 0.01) and PI 3-kinase of L6 neurons (*P = 0.02) of diabetic rats with nonsignificant trends in the same direction for RAGE, α2δ-1, and NF-κB (sample sizes for HSP27 controls = 5L3, 4L6; diabetic = 5L3, 5L6; for PI 3-kinase controls = 5L3, 6L6; diabetic = 5L3, 5L6; for RAGE controls = 3L3, 6L6; diabetic = 7L3, 5L6; for α2δ-1 controls = 3L3, 6L6; diabetic = 5L3, 5L6; for NF-κB controls = 5L3, 3L6; diabetic = 7L3, 5L6). *B*: Profile counts of neurons expressing HSP27, RAGE, or NF-κB in the L5 DRG. There were no significant differences in the percentage of neurons with low-, medium-, or high-level expression between diabetic ZDF and nondiabetic rats. For NF-κB, the percentage of all nuclei that were labeled is indicated (see caveat concerning percent-positive nuclei in RESEARCH DESIGN AND METHODS) and the percentage of neurons in which cytoplasmic labeling was identified is indicated (n = 4/group). *C*: Examples of L5 DRG sensory neurons expressing HSP27, RAGE, and NF-κB. Bar = 50 μm.

only been consistently identified in STZ mouse models (4,27).

In previous investigations , Oltman et al. (11) compared ZDF, lean littermates and also the Zucker parent strain that develops insulin resistance, hypertension, and dyslipidemia without hyperglycemia. ZDF diabetic rats had declines in motor nerve conduction velocity, declines in nerve blood flow, and changes in epineurial arteriole vascular relaxation. Insulin levels in the ZDF rats were four to five times that in lean controls and remained elevated to at least three times normal levels by ~30 weeks of age, an age comparable with our end point measures of insulin receptors and IRS. Although we did not measure insulin levels, these data were obtained on rats from the identical supplier and strain (Charles River). They indicate that our findings in insulin signal transduction molecules occurred in the setting of elevated, not reduced, insulin levels.

Several papers have also addressed other type 2 diabetic models in rats and mice. The BBZDR/Wor rat (9) had more mild electrophysiological changes and structural changes of nerves than related BB/Wor type 1 rats despite similar levels and durations of hyperglycemia. Furthermore, type 2 models have included the TSOD mouse exhibiting severe axon and myelin changes after 14 months of diabetes (28); the Goto-Kakizaki (GK) rat that demonstrated motor nerve conduction slowing, mild axonal atrophy, low-level demyelination, and axonal degeneration at 18 but not 2 months of diabetes (29); the *db/db* mouse with slowed sciatic nerve conduction velocity, axonal atrophy, and epidermal axon fiber loss up to 6 months of age (30,31); and the leptin-deficient (*ob/ob*) mouse with motor nerve conduction slowing, thermal hyperalgesia, mechanical allodynia, and loss of epidermal axons at 11 weeks of age (32).

The diabetic rats exhibited substantial mechanical allodynia without evidence of thermal hyperalgesia. Although controversial, several investigators have found a similar pattern of more robust mechanical allodynia than thermal hyperalgesia (33,34). Courteix et al. (35) observed thermal hyperalgesia at 4 weeks in STZ-induced diabetic rats but analyzed tail immersion, potentially targeting more distal tail cutaneous axons. Calcutt (36) has argued that some of these discrepancies may arise from testing methodology and the duration of diabetes. Dobretsov et al. (37) have suggested that hyperalgesia may relate better to impaired insulin signaling than hyperglycemia. In the current study, despite a long-term end point (4 months), pain behavior had not disappeared in favor of simple sensory loss, despite significant but incomplete epidermal denervation. By contrast, the long-term STZ-induced diabetic mouse models exhibit earlier mechanical and thermal hyperalgesia eventually followed by loss of sensation (27), and a separate investigation of ZDF rats identified loss of thermal sensation, albeit with a different food source and a slightly longer duration (28 weeks compared with 24 weeks) (21). Thus, we think it unlikely that thermal testing and mechanical testing have inherently different sensitivity. Thermal stimuli do, however, penetrate more deeply than the epidermis and may trigger responses from dermal nociceptive afferents that are better preserved.

We also noted a trend toward upregulation of mRNAs for the α2δ-1 calcium channel subunit, an auxiliary voltage-gated calcium channel protein that modulates calcium channel activity and is widely expressed in most DRG sensory neurons (38). This is particularly relevant given the binding of gabapentin and pregabalin to this channel in mediating analgesia during neuropathic pain (39). Other specific ion channels linked to diabetic neuropathic pain not examined here include Cav3.2 T-type calcium channels and several sodium channels: Nav1.3 (upregulation), Nav1.7 (upregulation, increased tyrosine phosphorylation), Nav1.6 and Nav1.8 (both downregulated but with increased serine/threonine phosphorylation; Nav 1.6 also had increased tyrosine phosphorylation) (40), Nav1.9 (upregulated), and β3 (upregulated) (41,42).

Sural myelinated axon counts did not identify evidence of more proximal perikaryal or axon dropout. In the skin, however, we provide evidence of both dermal and epidermal axon loss. Epidermal axon loss has been described in several DPN models, including the long-term STZ-induced diabetic mouse (3,43); dermal loss has only been reported previously in mice, along with loss of Merkel cells (44,45). We deliberately investigated larger calibre axons that express the neurofilament marker and confirmed that DPN is not exclusively confined to small axons in this type 2

model. Although microvascular changes are a recognized feature of ZDF rats, we chose not to emphasize its role in DPN in this work. Changes in nerve blood flow do not provide a satisfying explanation of the phenotype identified, and the issue has been extensively discussed elsewhere (46).

We chose quantitative RT-PCR as a sensitive measure of early changes that might exist in the mRNA population in lumbar DRG in response to diabetes. Quantitative RT-PCR can be extraordinarily sensitive to artifact such that we chose several types of controls. Samples without expression of a HKG were excluded, and because diabetes might alter HKG expression, we chose two separate markers not known to be altered by diabetes: 18S rRNA and cyclophilin, emphasizing the latter. We were skeptical of results with a less than twofold change in expression. Although we might expect L3 and L6 ganglia (L5 were used for immunohistochemistry, and we did not pool ganglia, an approach sometimes used) to show parallel changes in expression, they do have different innervation territories, a possible reason for different patterns of change. It is important to recognize that mRNA changes, especially mild ones, may simply represent trends in gene expression without changes in overall protein content. The overall changes that we observed in mRNA levels and protein were concordant: mild trends toward mRNA upregulation but generally preserved proportions of protein expression in neurons.

Our list of molecules was highly selected based on previous work in type 1 models, but each had a specific rationale. We had the most confidence in the changes seen in IRS-2 and HSP27 because the direction of change was consistent in both ganglia, greater than twofold, seen with two HKGs, and statistically significant in at least one ganglia level. Regrettably, we did not have a suitable antibody to address protein expression of IRS-2, whereas HSP27 protein expression was observed in a similar proportion of sensory neurons between diabetic and control animals. In previous work, we have identified rises in HSP27 mRNA by ISH in long-term type 1 STZ-induced diabetic rats and by immunohistochemistry in motor neurons of type 1 diabetic mice (2,4).

HSP27 is a molecular chaperone that refolds of denatured proteins and promotes the survival of injured neurons. It does this by inhibiting cytochrome c–mediated apoptosis (47), stabilizing mRNA, and stabilizing the neuron cytoskeleton (48,49).

Overall, our ZDF rats had relatively mild DPN, without declines in mRNAs for Nf200 or calcitonin gene-related peptide, features of type 1 models (2,50). Had our ZDF rats been taken out to longer time points, it seems possible that these critical structural proteins would have been altered by diabetes. This would be a difficult undertaking, however, because ZDF rat mortality significantly rises by the 4- to 5-month time point evaluated in this study.

The preservation and trends toward upregulation of insulin signal transduction machinery illustrate that such pathways remain available for input despite the gradual loss of ligand known to occur with pancreatic β-cell failure. The upregulation of IRβ resembles the changes noted in other type 1 models of DPN in which ligand deficiency may play a role in inducing a counter-regulatory enhancement of insulin receptor expression. Alternatively, axotomized axons also upregulate their expression of IRβ, and the trend toward change may reflect a response to distal axon loss. It is uncertain whether the rises in IRβ and IRS-2 that we observed contribute to or compensate for neuronal abnormalities.

ACKNOWLEDGMENTS

D.W.Z. is supported as a Scientist of the Alberta Heritage Foundation for Medical Research (AHFMR). The work was supported by the Canadian Institutes of Health Research, the Canadian Diabetes Association, and the AHFMR.

Brenda Boake provided expert secretarial assistance.

REFERENCES

1. Wild S, Roglic G, Green A, Sicree R, King H: Global prevalence of diabetes: estimates for the year 2000 and projections for 2030. *Diabetes Care* 27:1047–1053, 2004
2. Zochodne DW, Verge VMK, Cheng C, Sun H, Johnston J: Does diabetes target ganglion neurones? Progressive sensory neurone involvement in long-term experimental diabetes. *Brain* 124:2319–2334, 2001
3. Kennedy JM, Zochodne DW: Experimental diabetic neuropathy with spontaneous recovery: is there irreparable damage? *Diabetes* 54:830–837, 2005
4. Ramji N, Toth C, Kennedy J, Zochodne DW: Does diabetes mellitus target motor neurons? *Neurobiol Dis* 26:301–311, 2007
5. Scott JN, Clark AW, Zochodne DW: Neurofilament and tubulin gene expression in progressive experimental diabetes: failure of synthesis and export by sensory neurons. *Brain* 122:2109–2118, 1999
6. Yagihashi S, Kamijo M, Watanabe K: Reduced myelinated fiber size correlates with loss of axonal neurofilaments in peripheral nerve of chronically streptozotocin diabetic rats. *Am J Pathol* 136:1365–1373, 1990
7. Kamiya H, Zhangm W, Sima AA: Apoptotic stress is counterbalanced by survival elements preventing programmed cell death of dorsal root ganglions in subacute type 1 diabetic BB/Wor rats. *Diabetes* 54:3288–3295, 2005
8. Cheng C, Zochodne DW: Sensory neurons with activated caspase-3 survive long-term experimental diabetes. *Diabetes* 52:2363–2371, 2003
9. Sima AA, Zhang W, Xu G, Sugimoto K, Guberski D, Yorek MA: A comparison of diabetic polyneuropathy in type II diabetic BBZDR/Wor rats and in type I diabetic BB/Wor rats. *Diabetologia* 43:786–793, 2000
10. Li F, Abatan OI, Kim H, Burnett D, Larkin D, Obrosova IG, Stevens MJ: Taurine reverses neurological and neurovascular deficits in Zucker diabetic fatty rats. *Neurobiol Dis* 22:669–676, 2006
11. Oltman CL, Coppey LJ, Gellett JS, Davidson EP, Lund DD, Yorek MA: Progression of vascular and neural dysfunction in sciatic nerves of Zucker diabetic fatty and Zucker rats. *Am J Physiol Endocrinol Metab* 289:E113–E122, 2005
12. Brussee V, Cunningham FA, Zochodne DW: Direct insulin signaling of neurons reverses diabetic neuropathy. *Diabetes* 53:1824–1830, 2004
13. Singhal A, Cheng C, Sun H, Zochodne DW: Near nerve local insulin prevents conduction slowing in experimental diabetes. *Brain Res* 763:209–214, 1997
14. Sugimoto K, Murakawa Y, Zhang W, Xu G, Sima AA: Insulin receptor in rat peripheral nerve: its localization and alternatively spliced isoforms. *Diabete Metab Res Rev* 16:354–363, 2000
15. Sugimoto K, Murakawa Y, Sima AA: Expression and localization of insulin receptor in rat dorsal root ganglion and spinal cord. *J Peripher Nerv Syst* 7:44–53, 2002
16. Friedman JE, de Vente JE, Peterson RG, Dohm GL: Altered expression of muscle glucose transporter GLUT-4 in diabetic fatty Zucker rats (ZDF/Drt-fa). *Am J Physiol* 261:E782–E788, 1991
17. Clark JB, Palmer CJ, Shaw WN: The diabetic Zucker fatty rat. *Proc Soc Exp Biol Med* 173:68–75, 1983
18. Phillips MS, Liu Q, Hammond HA, Dugan V, Hey PJ, Caskey CJ, Hess JF: Leptin receptor missense mutation in the fatty Zucker rat. *Nat Genet* 13:18–19, 1996
19. Chen D, Wang MW: Development and application of rodent models for type 2 diabetes. *Diabetes Obes Metab* 7:307–317, 2005
20. Shibata T, Takeuchi S, Yokota S, Kakimoto K, Yonemori F, Wakitani K: Effects of peroxisome proliferator-activated receptor-alpha and -gamma agonist, JTT-501, on diabetic complications in Zucker diabetic fatty rats. *Br J Pharmacol* 130:495–504, 2000
21. Oltman CL, Davidson EP, Coppey LJ, Kleinschmidt TL, Lund DD, Adebara ET, Yorek MA: Vascular and neural dysfunction in Zucker diabetic fatty rats: a difficult condition to reverse. *Diabetes Obes Metab* 10:64–74, 2008
22. Shimoshige Y, Ikuma K, Yamamoto T, Takakura S, Kawamura I, Seki J, Mutoh S, Goto T: The effects of zenarestat, an aldose reductase inhibitor,

on peripheral neuropathy in Zucker diabetic fatty rats. *Metabolism* 49: 1395–1399, 2000
23. Schmidt RE, Dorsey DA, Beaudet LN, Peterson RG: Analysis of the Zucker diabetic fatty (ZDF) type 2 diabetic rat model suggests a neurotrophic role for insulin/IGF-I in diabetic autonomic neuropathy. *Am J Pathol* 163:21–28, 2003
24. Hargreaves K, Dubner R, Brown F, Flores C, Joris J: A new and sensitive method for measuring thermal nociception in cutaneous hyperalgesia. *Pain* 32:77–88, 1988
25. Fernyhough P, Smith DR, Schapansky J, Van Der Ploeg R, Gardiner NJ, Tweed CW, Kontos A, Freeman L, Purves-Tyson TD, Glazner GW: Activation of nuclear factor-kappaB via endogenous tumor necrosis factor alpha regulates survival of axotomized adult sensory neurons. *J Neurosci* 25:1682–1690, 2005
26. Lewis SE, Mannion RJ, White FA, Coggeshall RE, Beggs S, Costigan M, Martin JL, Dillmann WH, Woolf CJ: A role for HSP27 in sensory neuron survival. *J Neurosci* 19:8945–8953, 1999
27. Toth C, Rong LL, Yang C, Martinez JA, Song F, Ramji N, Brussee V, Liu W, Durand J, Nguyen MD, Schmidt AM, Zochodne DW: Receptor for advanced glycation end products (RAGE) and experimental diabetic neuropathy. *Diabetes* 57:1002–1017, 2008
28. Iizuka S, Suzuki W, Tabuchi M, Nagata M, Imamura S, Kobayashi Y, Kanitani M, Yanagisawa T, Kase Y, Takeda S, Aburada M, Takahashi KW: Diabetic complications in a new animal model (TSOD mouse) of spontaneous NIDDM with obesity. *Exp Anim* 54:71–83, 2005
29. Murakawa Y, Zhang W, Pierson CR, Brismar T, Ostenson CG, Efendic S, Sima AA: Impaired glucose tolerance and insulinopenia in the GK-rat causes peripheral neuropathy. *Diabete Metab Res Rev* 18:473–483, 2002
30. Underwood RA, Gibran NS, Muffley LA, Usui ML, Olerud JE: Color subtractive-computer-assisted image analysis for quantification of cutaneous nerves in a diabetic mouse model. *J Histochem Cytochem* 49:1285–1291, 2001
31. Norido F, Canella R, Zanoni R, Gorio A: Development of diabetic neuropathy in the C57BL/Ks (db/db) mouse and its treatment with gangliosides. *Exp Neurol* 83:221–232, 1984
32. Drel VR, Mashtalir N, Ilnytska O, Shin J, Li F, Lyzogubov VV, Obrosova IG: The leptin-deficient (ob/ob) mouse: a new animal model of peripheral neuropathy of type 2 diabetes and obesity. *Diabetes* 55:3335–3343, 2006
33. Fox A, Eastwood C, Gentry C, Manning D, Urban L: Critical evaluation of the streptozotocin model of painful diabetic neuropathy in the rat. *Pain* 81:307–316, 1999
34. Romanovsky D, Cruz NF, Dienel GA, Dobretsov M: Mechanical hyperalgesia correlates with insulin deficiency in normoglycemic streptozotocin-treated rats. *Neurobiol Dis* 24:384–394, 2006
35. Courteix C, Eschalier A, Lavarenne J: Streptozocin-induced diabetic rats: behavioural evidence for a model of chronic pain. *Pain* 53:81–88, 1993
36. Calcutt NA: Experimental models of painful diabetic neuropathy. *J Neurol Sci* 220:137–139, 2004
37. Dobretsov M, Ghaleb AH, Romanovsky D, Pablo CS, Stimers JR: Impaired insulin signaling as a potential trigger of pain in diabetes and prediabetes. *Int Anesthesiol Clin* 45:95–105, 2007
38. Cole RL, Lechner SM, Williams ME, Prodanovich P, Bleicher L, Varney MA, Gu G: Differential distribution of voltage-gated calcium channel alpha-2 delta (alpha2delta) subunit mRNA-containing cells in the rat central nervous system and the dorsal root ganglia. *J Comp Neurol* 491:246–269, 2005
39. Sills GJ: The mechanisms of action of gabapentin and pregabalin. *Curr Opin Pharmacol* 6:108–113, 2006
40. Hong S, Morrow TJ, Paulson PE, Isom LL, Wiley JW: Early painful diabetic neuropathy is associated with differential changes in tetrodotoxin-sensitive and -resistant sodium channels in dorsal root ganglion neurons in the rat. *J Biol Chem* 279:29341–29350, 2004
41. Craner MJ, Klein JP, Renganathan M, Black JA, Waxman SG: Changes of sodium channel expression in experimental painful diabetic neuropathy. *Ann Neurol* 52:786–792, 2002
42. Shah BS, Gonzalez MI, Bramwell S, Pinnock RD, Lee K, Dixon AK: Beta3, a novel auxiliary subunit for the voltage gated sodium channel is upregulated in sensory neurones following streptozocin induced diabetic neuropathy in rat. *Neurosci Lett* 309:1–4, 2001
43. Bianchi R, Buyukakilli B, Brines M, Savino C, Cavaletti G, Oggioni N, Lauria G, Borgna M, Lombardi R, Cimen B, Comelekoglu U, Kanik A, Tataroglu C, Cerami A, Ghezzi P: Erythropoietin both protects from and reverses experimental diabetic neuropathy. *Proc Natl Acad Sci U S A* 101:823–828, 2004
44. Christianson JA, Ryals JM, Johnson MS, Dobrowsky RT, Wright DE: Neurotrophic modulation of myelinated cutaneous innervation and mechanical sensory loss in diabetic mice. *Neuroscience* 145:303–313, 2007
45. Christianson JA, Riekhof JT, Wright DE: Restorative effects of neurotrophin treatment on diabetes-induced cutaneous axon loss in mice. *Exp Neurol* 179:188–199, 2003
46. Zochodne DW: Nerve and ganglion blood flow in diabetes: an appraisal. In *Neurobiology of Diabetic Neuropathy.* Int. Rev. Neurobiol. Tomlinson D, Ed. San Diego, Academic Press, 2002, p. 161–202
47. Murashov AK, Ul Haq I, Hill C, Park E, Smith M, Wang X, Goldberg DJ, Wolgemuth DJ: Crosstalk between p38, Hsp25 and Akt in spinal motor neurons after sciatic nerve injury. *Brain Res Mol Brain Re* 93:199–208, 2001
48. Benn SC, Perrelet D, Kato AC, Scholz J, Decosterd I, Mannion RJ, Bakowska JC, Woolf CJ: Hsp27 upregulation and phosphorylation is required for injured sensory and motor neuron survival. *Neuron* 36:45–56, 2002
49. Costigan M, Mannion RJ, Kendall G, Lewis SE, Campagna JA, Coggeshall RE, Meridith-Middleton J, Tate S, Woolf CJ: Heat shock protein 27: developmental regulation and expression after peripheral nerve injury. *J Neurosci* 18:5891–5900, 1998
50. Fernyhough P, Diemel LT, Brewster WJ, Tomlinson DR: Deficits in sciatic nerve neuropeptide content coincide with a reduction in target tissue nerve growth factor messenger RNA in streptozotocin-diabetic rats: effects of insulin treatment. *Neuroscience* 62:337–344, 1994